ADVANCED OPTICAL MATERIALS
www.advopticalmat.de

Thermal Tuning of Surface Plasmon Polaritons Using Liquid Crystals

*Arif E. Cetin, Alket Mertiri, Min Huang, Shyamsunder Erramilli, and Hatice Altug**

Nanoplasmonics provides a method to manipulate and control light at metal surfaces below the diffraction limit by surface plasmons, which are collective electron oscillations generated by the coupling with an incident light at a metal–dielectric interface.[1,2] Plasmonic metamaterials can be engineered for different functionalities that have led to demonstrations of novel concepts such as optical cloaking, superlensing, nonlinear photonics and optical waveguides[3–9] as well as photonic components, i.e., optical switches, filters, and lenses.[10–19] Compared to the prediction of the classical aperture theory, orders of magnitude larger transmission have been demonstrated through subwavelength plasmonic nano-apertures with the excitation of surface plasmon grating orders.[20] Extremely large near-field enhancements have been shown through plasmonic systems with nanometer-scale openings.[21–24]

Despite their widespread applications, controlling the optical responses of plasmonic systems is challenging. One method to control the plasmonic responses is to vary the geometrical shape or the properties of the constituent materials. However, this method is static and limits the flexibility when integrating these passive plasmonic components into complex systems. Therefore, there is a strong need for active plasmonic devices enabling dynamical tuning of the optical properties through external control mechanisms. Manipulation of the refractive index of the medium in the vicinity of the plasmonic system is promising to achieve dynamic tuning. As surface plasmons propagate along metal surfaces (surface plasmon polaritons) or localize at metallic features (localized surface plasmons), they are highly sensitive to the changes in the local refractive index. Hence, dynamically modifying the refractive index can actively tune the spectral response of the plasmonic systems. Liquid crystals are ideal candidates due to their exceptional tunable optical/electrical/thermal properties.[25,26] Their broad optical anisotropy derives from the anisotropic molecular alignments that are extremely sensitive to the external parameters such as light,[27,28] electric field[29–31] and temperature.[32,33] The tunability of liquid crystal properties has led to large variety of dynamic plasmonic applications. For example, photo-switchable gratings produced from liquid crystals can enable tuning of plasmonic interactions by an external pump light.[34] Electrical tuning of plasmonic properties of a system composed of periodic arrays of nanoholes or nanorods incorporating a liquid crystal medium can be achieved via an external voltage source.[35–40] Recently, a plasmonic Fano switch has been demonstrated using a plasmonic cluster supporting a Fano resonance, which is actively modulated through liquid crystals in the presence of a low-voltage external source.[41] The use of thermally controlled liquid crystals is an alternative way to modify the plasmonic properties.[42–44] Thermally controlled active plasmonic systems could enable much stronger and more efficient tuning capabilities as well as large spectral tuning ranges compared to photo-switchable or electrically tunable platforms.[45] Large refractive index variations can be achieved by precisely controlling the temperature in different liquid crystal phases. However, recently demonstrated thermally controlled plasmonic platforms show only ≈1–2 nm spectral tuning of localized surface plasmon modes.[27,28,32,33]

In this letter, we introduce an active plasmonic platform incorporating a highly sensitive plasmonic chip and a thermally controlled liquid crystal medium that is capable of large spectral tuning. Our platform consists of nanohole arrays fabricated through gold films. This plasmonic substrate enables extraordinary light transmission, which is exceptionally sensitive to the changes in the local refractive index as it supports highly accessible large local fields. Introducing a liquid crystal medium, we show that the transmission resonance supported by the nanohole arrays can be thermally tuned by applying an external heat source. Our platform is capable of high contrast change in the effective refractive index of the medium in the vicinity of the plasmonic arrays. Varying the temperature within the nematic phase from 15 to 33 °C, we demonstrate a refractive index change as large as ≈0.0317. Consequently, our platform enables a tuning of plasmonic wavelength as large as ≈19 nm. The ability to control the order of liquid crystal molecules from nematic to isotropic phase provides an efficient way of spectral tuning. At the phase transition temperature, more than 12 nm shift is achieved via changing the temperature by only ≈1 °C corresponding to a refractive index change of ≈0.02.

A. E. Cetin, Dr. M. Huang, Dr. H. Altug
Department of Electrical and Computer Engineering
Boston University
Boston, Massachusetts, 02215, USA
A. Mertiri, Dr. S. Erramilli, Dr. H. Altug
Division of Materials Science and Engineering
Boston University
Boston, Massachusetts, 02215, USA
Dr. S. Erramilli
Department of Physics
Boston University
Boston, Massachusetts, 02215, USA
A. E. Cetin, Dr. H. Altug
Bioengineering Department
Ecole Polytechnique Federale de Lausanne (EPFL)
Lausanne, CH-1015, Switzerland
E-mail: hatice.altug@epfl.ch

DOI: 10.1002/adom.201300303

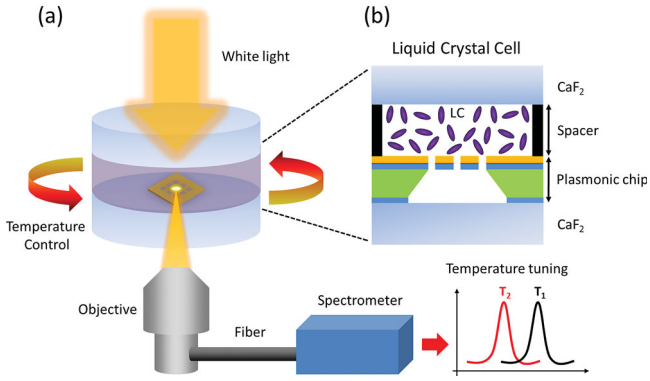

Figure 1. a) Schematic view of the experimental setup containing a liquid crystal (LC) cell thermally controlled by a heat bath, white light incident source collected by an objective lens and a spectrometer collecting the plasmonic response for different temperature values. b) Zoomed schematic of the liquid crystal cell between the upper CaF_2 window and the plasmonic chip.

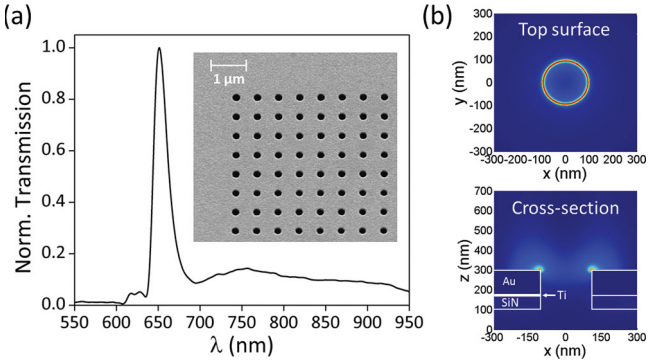

Figure 2. a) Experimental far-field response of the nanohole array under an unpolarized light source. Figure inset shows the scanning electron microscope image of the fabricated nanohole array through gold film by deep-ultraviolet lithography. b) Calculated near-field response of the nanohole array at the top surface (air–gold interface) and through cross-section. For gold nano-apertures, hole diameter = 200 nm and period of the array = 600 nm.

The experimental setup is shown in **Figure 1**a. Here, the plasmonic chip interfacing with a liquid crystal medium is inserted between two calcium fluoride (CaF_2) windows. The temperature is controlled via a heat bath that circulates water through a homemade sample cell and measured using a thermocouple. In order to create the liquid crystal cell, a 50 μm thick Maylar spacer is used between the plasmonic chip and the upper CaF_2 window as shown in the zoomed image (Figure 1b). Optical characterization is done through spectroscopy measurement by using an unpolarized white light source. Transmitted light from the plasmonic chip is collected by a high-magnification objective lens (Nikon Objectives with 100× magnification and NA: 0.6 embedded in Nikon Eclipse-Ti microscope) coupled into an optical fiber and then recorded using a spectrometer (SpectraPro 500i with 1 nm spectral resolution).

Our active tuning platform is based on the extraordinary light transmission phenomenon via nanohole arrays fabricated through a metal film. The extraordinary transmission resonances exist at specific wavelengths where the grating coupling conditions are met. At these grating wavelengths, the normally incident light is coupled to surface plasmons.[21,46] These transmission resonances highly depend on the refractive index of the surrounding medium. In our platform, we use plasmonic nanohole arrays with a diameter of 200 nm and an array period of 600 nm. Nanoholes through 125 nm thick gold film are manufactured via a fabrication process based on deep ultraviolet lithography. Inset in **Figure 2**a shows the scanning electron microscope image of the fabricated nanoholes which are well defined and uniform. Compare to current electron beam lithography technique where each array is fabricated sequentially, this method is highly advantageous for fabrication of nanoapertures at wafer scale in a low cost and time effective way by enabling parallel fabrication of nanoapertures in a lift-off free manner (see Supporting Information text and Figure S1 for fabrication details).[21,46–49]

Figure 2a shows the experimental far-field response of the nanohole array under normally incident unpolarized light source. Strong transmission resonance located at 652 nm is the mode which will be thermally controlled in the following section. This mode is due to the surface plasmon excitation corresponding to (–1,0) grating order of the square lattice. We have analyzed the optical response of this mode in detail in our earlier work.[21] The mode has a dipolar character where the light couples to localized surface plasmons resulting in strong light transmission and large local electromagnetic fields in the vicinity of the nanohole array. Under an unpolarized light source, highly enhanced near-fields strongly localize around the rims of the nanoholes as shown by the electric field intensity distribution (Figure 2b) calculated at the top surface of the metal. The cross-sectional profile also indicates that local fields extensively extend into the surrounding medium. By providing these accessible and large local fields, the nanoaperture system is highly sensitive to the changes in the local refractive index. Therefore, our plasmonic substrate is highly advantageous for spectral tuning applications via modification of the surrounding medium. In the following section, we describe the use of a liquid crystal medium for thermally varying the local refractive index around the plasmonic chip to spectrally tune this dipolar transmission resonance.

Thermal modulation of the effective refractive index of the medium in the vicinity of the plasmonic chip is achieved by using 4-cyano-4′-pentylbiphenyl (5CB) liquid crystal (see Supporting Information text and Figure S2 for the thermal properties of 5CB). UV–vis–NIR spectrum of a 50 μm thick 5CB liquid crystal sample (see Figure S2c) shows no absorbance peaks in our wavelength range that might interfere with the plasmonic mode. **Figure 3**a and b show the variation in the transmission resonance and the spectral position of it for different temperatures, respectively. In the presence of the liquid crystal that increases the refractive index around the bare aperture, the plasmonic mode red-shifts from ≈651 nm to ≈1027 nm at 15 °C. The transmission resonance supported by the nanohole arrays can be spectrally tuned over ≈18 nm (from ≈1027.1 ±1 nm to ≈1008.4 ± 1 nm) between 15 °C and 33 °C where the liquid crystal shows nematic (*N*) molecular order. Toward the transition temperature T_c, the average refractive

Adv. Optical Mater. **2013**,
DOI: 10.1002/adom.201300303

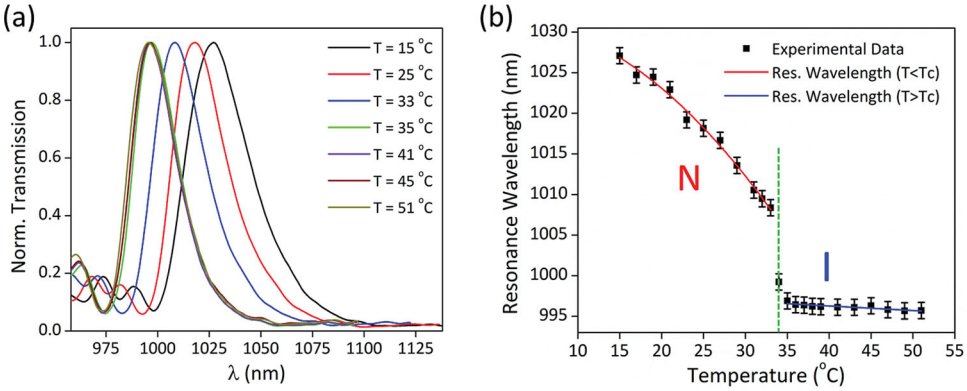

Figure 3. a) Experimental transmission response of the nanohole array for different temperatures from 15 °C to 51 °C. b) Spectral position of the transmission resonance for different temperatures. In the figure, the red curve denotes the resonance points below the transition temperature T_c (showing the quadratic behavior) and the blue curve denotes the points above T_c (showing the linear behavior). The green dashed line represents the transition between nematic (*N*) and isotropic (*I*) phases.

index of 5CB gradually decreases[50,51] that results in consecutive blue-shifts in the plasmonic mode. As shown in Figure 3b for this temperature range, the resonance wavelength has a quadratic relationship with temperature denoted by a red curve. Around the temperature T_c where the transition occurs from the nematic phase to isotropic phase (*I*), we observe a sharp shift in the transmission resonance with only 1 °C change, from ≈1008 nm to ≈996 nm, relating to the rapid decrease of the average refractive index of 5CB. Above temperature T_c, refractive index of 5CB shows minor variations and the transmission resonance slowly blue-shifts with temperature. For this range, the transmission resonance shows a linear dependence on the temperature as denoted by a blue curve in Figure 3b. We also successfully demonstrate the reproducibility of our thermal tuning capability via three independent experiments in Supporting Information Figure S3.

The resonance wavelength strongly depends on the refractive index of the liquid crystal medium covering the plasmonic substrate. In order to show how strongly we can tune the effective refractive index with temperature, we represent the liquid crystal medium as a bulk dielectric. We determine the effective refractive index of the liquid crystal medium, n_{eff}(LC) from the relationship between the spectral position of the plasmonic mode (λ) and the refractive index of the homogeneous dielectric medium, n_{bulk} (schematically shown in **Figure 4**a) by measuring the optical response of the nanohole array in different bulk solutions. Figure 4b shows the spectral response of the nanohole array at room temperature (T = 20 °C) in different refractive indices including de-ionized (DI) water (n = 1.3325), acetone (n = 1.3591), ethanol (n = 1.3616), isopropyl alcohol (n = 1.3776) and glycerol (n = 1.4722). Obtaining the spectral position of the transmission resonance, we determine a linear relationship between the resonance wavelength of the plasmonic mode and the refractive index of the bulk solution, $\lambda = 589.62 n_{bulk} + 62.005$ (Figure 4c). Using this spectral relationship, we calculate the effective refractive indices of the liquid crystal, n_{eff}(LC) at the corresponding resonance wavelength, λ for different temperatures. Varying the temperature from 15 °C to 33 °C, we achieve a dynamic range of ≈0.0317 from n_{eff} (LC at 15 °C) = 1.6368 ± 0.00169 to n_{eff} (LC at 33 °C) = 1.6051 ± 0.00169. Figure 4d shows that the calculated effective refractive index of the medium in the vicinity of the plasmonic nanoapertures follows the trend of the average refractive index of 5CB.[50,51] This is due to the fact that we utilize a bulk liquid crystal substrate in our tuning platform which causes the refractive index of the medium to be the average of ordinary and extraordinary refractive indices of 5CB. Between 15 °C and 33 °C, the effective (or average) refractive index decreases quadratically with the temperature. At the phase transition of the liquid crystal molecules between the nematic to the isotropic phase, the sharp variation in the refractive index of 5CB enables the tuning of the refractive index by ≈0.02 with a temperature change of only 1 °C. Above the nematic-isotropic transition temperature T_c, the refractive index changes slightly.

The presented platform provides a convenient way to tune the plasmonic properties in a large dynamic range as well as dramatic thermal responses via controlling the phases of the liquid crystal molecules. Such platform holds great promises for controlling surface plasmons thermally and the tunability of the liquid crystal molecules can be further improved to have much larger spectral shifts in the plasmonic modes. **Figure 5** shows the refractive indices at room temperature for the liquid crystal used in our study, 5CB measured at 633 nm by Li et al.[50] Here, the red and blue dots show the extraordinary (n_e) and ordinary (n_o) refractive indices below the transition temperature, respectively. Above the transition temperature, these indices converge ($n_o \approx n_e$) as denoted by the green dots. As seen in the Figure, 5CB has a high contrast between extraordinary and ordinary refractive indices, e.g., as large as 0.19 at room temperature. These effective indices depend on the orientation of the liquid crystal directors with respect to the polarization direction of the illumination light. A system that controls this orientation would result in a much larger index contrast, thus promising larger spectral tuning. In Figure 5, black squares demonstrate the calculated refractive index of the bulk 5CB using our refractive index/resonance wavelength relationship that we obtain from Figure 4d. In our plasmonic substrate, we utilize a bulk liquid

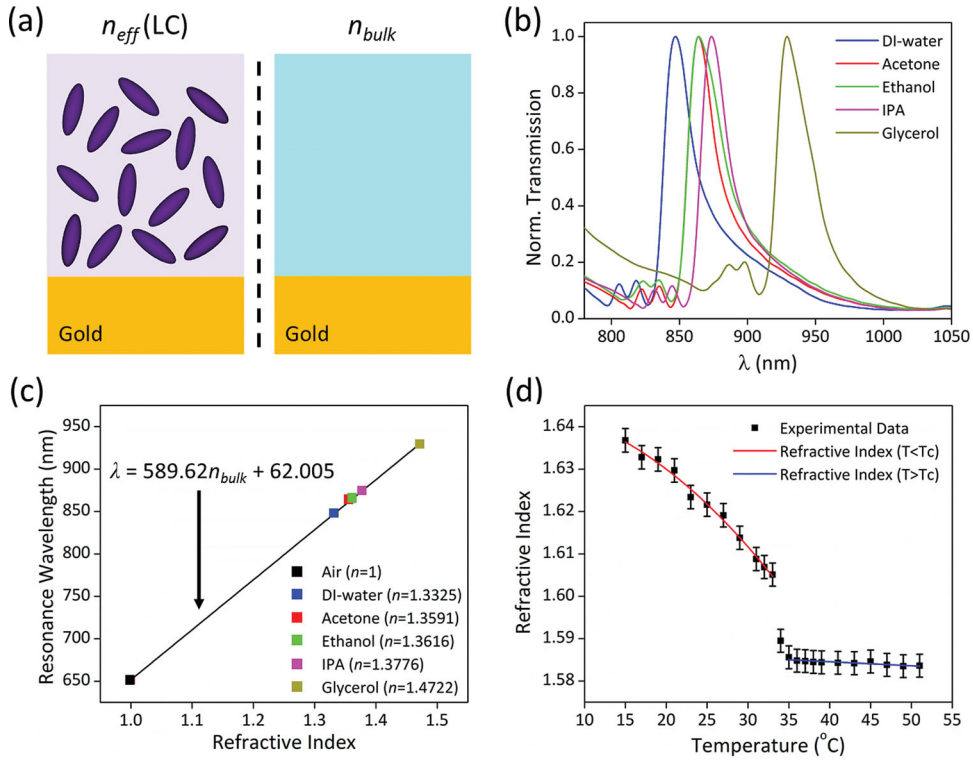

Figure 4. a) Schematic view of the plasmonic system embedded in a liquid crystal medium having an average refractive index, n_{eff} (LC) represented by a bulk homogeneous dielectric medium with a refractive index, n_{bulk}. b) Experimental transmission response of the nanohole array for different refractive indices of bulk solutions, DI water (n = 1.3325), acetone (n = 1.3591), ethanol (n = 1.3616), isopropyl alcohol (IPA) (n = 1.3776) and glycerol (n = 1.4722). c) Linear relationship between the resonance wavelength of the plasmonic mode, λ, and the refractive index of the bulk solutions, n_{bulk}. d) Effective refractive index of the liquid crystal medium in the near-field of the nanohole array calculated from the linear relationship shown in Figure 4c. Here, the red curve denotes the refractive indices below the transition temperature, T_c (showing the quadratic behavior) and the blue curve denotes the refractive indices above T_c (showing the linear behavior).

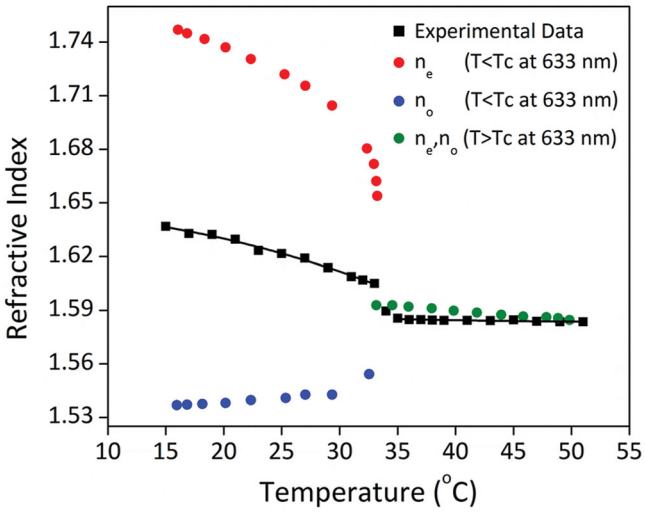

Figure 5. Ordinary, n_o (blue dots) and extraordinary, n_e (red dots) refractive indices of 5CB below the transition temperature. The refractive index, $n_o \approx n_e$ (green dots) above the transition temperature.[50] Black squares denote the average refractive index of 5CB calculated from the experimentally obtained resonance wavelength/refractive index relation.

crystal. Therefore, the orientation of the directors is in between extraordinary and ordinary axes resulting in an average refractive index between n_o and n_e. This average bulk refractive index does not vary with the polarization direction of the incident source as verified in Supporting Information Figure S4. The absence of the molecular order limits the spectral tunability, i.e., the refractive index changes in the nematic phase and at the phase transition are ≈0.0317 and ≈0.02, resulting in ≈18.7 nm and ≈12 nm shifts, respectively. The ability to control the liquid crystal director would result in a higher spectral tunability. For example, by ordering liquid crystal molecules along the extraordinary axis with n_e = 1.7562 at 15 °C followed by increasing the temperature to reach isotropic phase with n_o = 1.5929, as large as ≈96.3 nm spectral tuning can be achieved. Furthermore, as demonstrated by Figure 5, the slope of the index/temperature curve is sharper for individual ordinary (blue) and extraordinary (red) indices compared to the response of the bulk liquid crystal refractive index (black). Our work suggests that improved spectral tunability can be attained by appropriate surface treatment to control the molecular directors near the plasmonic device. Combining electro-optic methods with the thermal tuning by the application of directed electric fields would result in further control over spectral properties.[31,37,52]

Adv. Optical Mater. **2013**,
DOI: 10.1002/adom.201300303

In conclusion, we demonstrate a dynamically tunable plasmonic platform that enables spectrally large tuning capabilities. Our platform utilizes a thermally controlled liquid crystal medium and a plasmonic substrate composed of nanohole arrays. The system supports high sensitivities to surface conditions due to the large local electromagnetic fields at the plasmonic resonance. It enables a spectral tuning of resonance wavelength as large as ≈18.7 nm in a temperature range of 18 °C (through nematic phase) by overlapping these local fields with thermally controlled liquid crystal. Employing our active plasmonic system, we show the refractive index of the medium in the vicinity of the plasmonic substrate can be changed as large as ≈0.0317. The ability to thermally control the liquid crystal phases from nematic to isotropic where the strongest variations occur in the molecular orientation enables us to tune the spectral position of the plasmonic mode more than 12 nm in ≈1 °C temperature range.

Supporting Information

Supporting Information is available from the Wiley Online Library or from the author.

Acknowledgements

A. E. Cetin and A. Mertiri contributed equally to this work. Altug Research Group acknowledges National Science Foundation (NSF) CAREER Award and Presidential Early Career Award for Scientist and Engineers ECCS-0954790, Office of Naval Research (ONR) Young Investigator Award 11PR00755–00-P00001 and NSF Engineering Research Center on Smart Lighting EEC-0812056. Erramilli Research Group acknowledges support from National Institutes of Health (NIH) and the NSF. We thank Dr. Lynetta Meir for advice on simulations. We thank UCSB for their contribution in fabrication of the nanoapertures.

Received: July 22, 2013
Revised: September 17, 2013
Published online:

[1] J. S. Schuller, E. S. Barnard, W. Cai, Y. C. Jun, J. S. White, M. I. Brongersma, *Nat. Mater.* **2010**, *9*, 193.
[2] C. Genet, T. W. Ebbesen, *Nature* **2007**, *445*, 39.
[3] E. Ozbay, *Science* **2006**, *311*, 189.
[4] J. B. Pendry, *Phys. Rev. Lett.* **2000**, *85*, 3966.
[5] D. Schurig, J. J. Mock, B. J. Justice, S. A. Cummer, J. B. Pendry, A. F. Starr, D. R. Smith, *Science* **2006**, *314*, 977.
[6] S. Kim, J. Jin, Y. J. Kim, I. Y. Park, Y. Kim, S. W. Kim, *Nature* **2008**, *453*, 757.
[7] K. F. MacDonald, Z. L. Samson, M. I. Stockman, N. I. Zheludev, *Nat. Photonics* **2009**, *3*, 55.
[8] J. Butet, K. Thyagarajan, O. J. F. Martin, *Nano Lett.* **2013**, *13*, 1787.
[9] K. J. Savage, M. M. Hawkeye, R. Esteban, A. G. Borisov, J. Aizpurua, J. J. Baumberg, *Nature* **2012**, *491*, 574.
[10] S. A. Maier, P. G. Kik, H. A. Atwater, S. Meltzer, E. Harel, B. E. Koel, A. A. G. Requicha, *Nat. Mater.* **2003**, *2*, 229.
[11] Y. J. Liu, Q. Z. Hao, J. S. T. Smalley, J. Liou, I. C. Khoo, T. J. Huang, *Appl. Phys. Lett.* **2010**, *97*, 091101.
[12] H. J. Lezec, A. Degiron, E. Devaux, R. A. Linke, L. Martin-Moreno, F. J. Garcia-Vidal, T. W. Ebbesen, *Science* **2002**, *297*, 820.
[13] W. Srituravanich, L. Pan, Y. Wang, C. Sun, D. B. Bogy, X. Zhang, *Nat. Nanotechnol.* **2008**, *3*, 733.
[14] E. Cubukcu, E. A. Kort, K. B. Crozier, F. Capassoa, *Appl. Phys. Lett.* **2006**, *89*, 093120.
[15] K. Aydin, V. E. Ferry, R. M. Briggs, H. A. Atwater, *Nat. Commun.* **2011**, *2*, 517.
[16] R. Zia, M. L. Brongersma, *Nature Nanotechnol.* **2007**, *2*, 426.
[17] A. Kinkhabwala, Z. Yu, S. Fan, Y. Avlasevich, K. Mullen, W. E. Moerner, *Nat. Photonics* **2009**, *3*, 654.
[18] Y. J. Lu, J. Kim, H. Y. Chen, C. Wu, N. Dabidian, C. E. Sanders, C. Y. Wang, M. Y. Lu, B. H. Li, X. Qiu, W. H. Chang, L. J. Chen, G. Shvets, C. K. Shih, S. Gwo, *Science* **2012**, *337*, 450.
[19] I. Bulu, T. Babinec, B. Hausmann, J. T. Choy, M. Loncar, *Opt. Express* **2011**, *19*, 5268.
[20] T. W. Ebbesen, H. J. Lezec, H. F. Ghaemi, T. Thio, P. A. Wolff, *Nature* **1998**, *391*, 667.
[21] A. A. Yanik, A. E. Cetin, M. Huang, A. Artar, S. H. Mousavi, A. Khanikaev, J. H. Connord, G. Shvetsc, H. Altug, *Proc. Natl. Acad. Sci. USA* **2011**, *108*, 11784.
[22] A. E. Cetin, A. A. Yanik, C. Yilmaz, S. Somu, A. A. Busnaina, H. Altug, *Appl. Phys. Lett.* **2011**, *98*, 111110.
[23] R. Adato, A. A. Yanik, J. J. Amsden, D. L. Kaplan, F. G. Omenetto, M. K. Hong, S. Erramilli, H. Altug, *Proc. Natl. Acad. Sci. USA* **2009**, *106*, 19227.
[24] A. E. Cetin, H. Altug, *ACS Nano* **2012**, *6*, 9989.
[25] L. De Sio, A. Tedesco, S. Serak, N. Tabiryan, C. Umeton, *Mol. Cryst. Liq. Cryst.* **2012**, *560*, 143.
[26] M. Romito, L. De Sio, A. E. Vasdekis, C. Umeton, *Mol. Cryst. Liq. Cryst.* **2013**, *576*, 135.
[27] V. K. S. Hsiao, W. D. Kirkey, F. Chen, A. N. Cartwright, P. N. Prasad, T. J. Bunning, *Adv. Mater.* **2005**, *17*, 2211.
[28] V. K. S. Hsiao, Y. B. Zheng, B. K. Juluri, T. J. Huang, *Adv. Mater.* **2008**, *20*, 3528.
[29] M. Humar, M. Ravnik, S. Pajk, I. Musevic, *Nat. Photonics* **2009**, *3*, 595.
[30] W. Hu, H. Y. Zhao, L. Song, Z. Yang, H. Cao, Z. H. Cheng, Q. Liu, H. Yang, *Adv. Mater.* **2010**, *22*, 468.
[31] A. E. Cetin, O. E. Mustecaplioglu, *Phys. Rev. A* **2010**, *81*, 043812.
[32] A. N. G. Parra-Vasquez, L. Oudjedi, L. Cognet, B. Lounis, *J. Phys. Chem.* **2012**, *3*, 1400.
[33] A. Mertiri, T. Jeys, V. Liberman, M. K. Hong, J. Mertz, H. Altug, S. Erramilli, *Appl. Phys. Lett.* **2012**, *101*, 044101.
[34] Y. J. Liu, Y. B. Zheng, J. Liou, I. K. Chiang, I. C. Khoo, T. J. Huang, *J. Phys. Chem. C* **2011**, *115*, 7717.
[35] W. Dickson, G. A. Wurtz, P. R. Evans, R. J. Pollard, A. V. Zayats, *Nano Lett.* **2008**, *8*, 281.
[36] P. R. Evans, G. A. Wurtz, W. R. Hendren, R. Atkinson, W. Dickson, A. V. Zayats, R. J. Pollard, *Appl. Phys. Lett.* **2007**, *91*, 043101.
[37] A. E. Cetin, A. A. Yanik, A. Mertiri, S. Erramilli, O. E. Mustecaplioglu, H. Altug, *Appl. Phys. Lett.* **2012**, *101*, 121113.
[38] P. A. Kossyrev, A. Yin, S. G. Cloutier, D. A. Cardimona, D. Huang, P. M. Alsing, J. M. Xu, *Nano Lett.* **2005**, *5*, 1978.
[39] J. Berthelot, A. Bouhelier, C. Huang, J. Margueritat, G. Colas-des-Francs, E. Finot, J. C. Weeber, A. Dereux, S. Kostcheev, H. I. E. Ahrach, A. L. Baudrion, J. Plain, R. Bachelot, P. Royer, G. P. Wiederrecht, *Nano Lett.* **2009**, *9*, 3914.
[40] S. Khatua, W. S. Chang, P. Swanglap, J. Olson, S. Link, *Nano Lett.* **2011**, *11*, 3797.
[41] W. S. Chang, J. B. Lassiter, P. Swanglap, H. Sobhani, S. Khatua, P. Nordlander, N. J. Halas, S. Link, *Nano Lett.* **2012**, *12*, 4977.
[42] J. Xie, X. Zhang, Z. Peng, Z. Wang, T. Wang, S. Zhu, Z. Wang, L. Zhang, J. Zhang, B. Yang, *J. Phys. Chem. C* **2012**, *116*, 2720.

[43] G. M. Koenig Jr., M. V. Meli, J. S. Park, J. J. de Pablo, N. L. Abbott, *Chem. Mater.* **2007**, *19*, 1053.
[44] G. M. Koenig Jr., B. T. Gettelfinger, J. J. de Pablo, N. L. Abbott, *Nano Lett.* **2008**, *8*, 2362.
[45] G. Baffou, R. Quidant, *Laser & Photon. Rev.* **2013**, *7*, 171.
[46] A. Artar, A. A. Yanik, H. Altug, *Appl. Phys. Lett.* **2009**, *95*, 051105.
[47] T. Y. Chang, M. Huang, A. A. Yanik, H. Y. Tsai, P. Shi, S. Aksu, M. F. Yanik, H. Altug, *Lab Chip* **2011**, *11*, 3596.
[48] A. A. Yanik, M. Huang, O. Kamohara, A. Artar, T. W. Geisbert, J. H. Connor, H. Altug, *Nano Lett.* **2010**, *10*, 4962.
[49] K. Nakamoto, R. Kurita, O. Niwa, T. Fujii, M. Nishida, *Nanoscale* **2011**, *3*, 5067.
[50] J. Li, S. Gauza, S. T. Wu, *J. Appl. Phys.* **2004**, *96*, 19.
[51] R. G. Horn, *J. Phys. France* **1978**, *39*, 105.
[52] B. Maune, R. Lawson, C. Gunn, A. Scherer, L. Dalton, *Appl. Phys. Lett.* **2003**, *83*, 4689.

Adv. Optical Mater. **2013**,
DOI: 10.1002/adom.201300303